Journal of Molecular Structure 1108 (2016) 269–277

Contents lists available at ScienceDirect

Journal of Molecular Structure

journal homepage: http://www.elsevier.com/locate/molstruc

A fluorescent coumarin-thiophene hybrid as a ratiometric chemosensor for anions: Synthesis, photophysics, anion sensing and orbital interactions

Ufuk Yanar, Banu Babür, Damla Pekyılmaz, Issah Yahaya, Burcu Aydıner, Yavuz Dede*, Zeynel Seferoğlu**

Gazi University, Department of Chemistry, 06500 Ankara, Turkey

ARTICLE INFO

Article history:
Received 9 September 2015
Received in revised form
27 November 2015
Accepted 30 November 2015
Available online 11 December 2015

Keywords:
Coumarin
Coumarin-thiophene hybrid
Fluorescence chemosensor
Anion recognition
Frontier orbital
DFT

ABSTRACT

A colorimetric and fluorimetric fluorescent chemosensor (**CT-2**), having a coumarin ring as a signaling unit and an acetamido thiophene ring as an H-donor receptor, has been synthesized from amino derivative (**CT-1**) of **CT-2** for the purpose of recognition of anions in DMSO. The absorption and emission maxima were both determined for the fluorescent dye in different solvents. Both hypsochromic shift at the absorption maximum, and quenching of fluorescence after interactions between the anions and the receptoric part, were observed. This phenomenon was explained using orbital interactions based on quantum chemical calculations. The selectivity and sensitivity of **CT-2** for F^-, Cl^-, Br^-, I^-, AcO^-, CN^-, $H_2PO_4^-$, HSO_4^- and ClO_4^- anions were determined with spectrophotometric, fluorimetric and ^1H NMR titration techniques and it was found that **CT-2** be utilized for the detection of CN^-, F^- and AcO^- in the presence of other ions as competitors. Color and fluorescence changes visible to the naked eye and under UV (365 nm) were observed upon addition of CN^-, F^- and AcO^- to the solution of chemosensor (**CT-2**) in DMSO. The sensor showed no colorimetric and fluorimetric response for the anions such as Cl^-, Br^-, I^-, $H_2PO_4^-$, HSO_4^-, and ClO_4^-. However, ^1H NMR titration shows that the chemosensor was more sensitive to CN^-, than F^- and AcO^- at the stochiometric ratio of 1:2.5 respectively. Additionally, the compounds **CT-1** and **CT-2** showed good thermal stability for practical applications.

1. Introduction

Anions are important in clinical, environmental, chemical and industrial processes [1]. Drinking water is known to be the most important source of fluoride and so is important for both human body and bone growth [2]. Exposure to excess fluoride may cause collagen break down, bone disorder, thyroid activity, and depression. Fluoride deficiency causes gum disease and osteoporosis, while an excess (above 1.5 ppm) leads to fluorosis (fluoride poisoning) because of its nephrotoxic effect [3,4]. High chlorine concentration was determined in the sweat test used in the diagnosis of cystic fibrosis [5,6]. It is known that excess of bromide causes severe irritation of the respiratory tract. Iodide has an effect on the functioning of the thyroid gland. Both excess and deficiency of this anion affects the operation of the thyroid gland and can cause serious illness [7,8]. Acetate anion plays a critical role in many metabolic processes, and exhibits specific biochemical behavior on antibodies and enzymes [9,10]. Cyanide ion is also vital as a raw material in industrial process and it is also highly toxic for the human body [11,12].

As a consequence, efforts have been made to determine fluoride, chloride, bromide, iodide and other ions such as acetate, chlorate, sulfate, phosphate and cyanide in real samples. The determination of anions can be achieved by several methods including spectroscopic, chromatographic, electrochemical and analytical techniques. However, the detection of anions with the use of simple preparation and minimal instrumental assistance is desirable toward practical applications. Colorimetric and fluorimetric chemosensors are important alternatives to the traditional methods for determination of anions. Therefore, synthesis of new additional chemosensor is still required.

* Corresponding author.
** Corresponding author.
E-mail addresses: dede@gazi.edu.tr (Y. Dede), znseferoglu@gazi.edu.tr (Z. Seferoğlu).

http://dx.doi.org/10.1016/j.molstruc.2015.11.081
0022-2860/

The sensor **(CT-2)** reported here contains coumarin and thiophene unit as the main core. The coumarin ring is commonly used as a fluorophore/chromophore in sensor systems because of its high fluorescence quantum efficiency, large Stokes shift, bright color under ambient light and ease of synthesis and derivatization [13,14]. Thiophene derivatives are also valuable compounds in heterocyclic chemistry due to its important optical properties.

In this work we chose coumarin as the fluorophore/chromophore for signaling, and thiophene at the 3-position of the coumarin ring to modify the fluorescence properties of the coumarin core, in order to form a receptor for anions via an acetamide functional group. We first studied the photophysical properties of the fluorescence chemosensor **(CT-2)** and its starting compound **(CT-1)**. Afterwards, binding properties of the chemosensor toward specific anions such as F^-, Cl^-, Br^-, I^-, AcO^-, CN^-, $H_2PO_4^-$, HSO_4^- and ClO_4^- was also investigated. Additionally, the experimental results obtained were explained with theoretical calculations. Thermal properties of **CT-1** and **CT-2** for optical usage were also determined. **CT-2** showed remarkable selectivity toward CN^-, F^- and AcO^- over other anions at the stochiometric ratio of 1:5 (**CT-2**:Anion) respectively. However, the chemosensor was more sensitive to CN^-, than F^- and AcO^- at the stochiometric ratio of 1:2.5 respectively.

2. Experimental

2.1. Materials and instrumentations

All the chemicals used in the synthesis of the compounds were procured from Aldrich Chemical Company and were used without further purification. The solvents used were of spectroscopic grade. Thin-layer chromatography was carried out using precoated aluminium-backed plates (Merck Silica Gel 60 F254) and visualised under UV light ($\lambda = 254$–365 nm). FT-IR Spectra were recorded on a Mattson 1000 FT-IR spectrophotometer in KBr (υ are in cm^{-1}). NMR spectra were run on a Bruker Avance 300 MHz instrument. NMR samples were referenced against tetramethylsilane at 0.00 ppm for ^1H. Coupling constants (J) are given in hertz (Hz). Signals are abbreviated as follows: singlet, s; doublet, d; doublet–doublet, dd; triplet, t; multiplet, m. Chemical shifts (δ) are given in parts per-million (ppm) using the residue solvent peaks as reference relative to TMS. 'J' values are given in Hertz (Hz). High resolution mass spectra were recorded on a Waters-LCT-Premier-XE-LTOF (TOF-MS), mass spectrometer operated in Electronionization (EI) mode in m/z (rel. %) (Gazi University Laboratories, Department of Pharmacological Sciences). The melting points were measured using Electrothermal IA9200 apparatus and were uncorrected. Thermal analyses were performed with a Shimadzu DTG-60H system, up to 600 °C (10 °C min^{-1}) under a dynamic nitrogen atmosphere (15 mL min^{-1}).

2.2. Spectrophotometric measurements

Ultraviolet–visible (UV–vis) absorption spectra were recorded on Shimadzu Corporation, Kyoto Japan UV-1800 240 V spectrophotometer (Gazi University, Department of Chemistry, Turkey) at the wavelength of maximum absorption (λ_{max}, in nm). Fluorescence spectra were recorded on HITACHI F-7000 FL Spectrofluorophotometer. All spectrophotometric measurements were performed in thermostated quartz sample cells at 20 °C, using spectral grade solvents. The solution concentrations were 10 μM for absorption spectroscopy and 1.0–5.0 μM for fluorescence spectroscopy. Spectrophotometer slit widths were set to bandwidths of 5 nm for emission spectroscopy. The relative fluorescence quantum yields, Φ_{fl}, were determined by standard methods [15,16] with Coumarin 153 (laser grade, Acros Organics, $\Phi_{fl} = 0.38$ in ethanol) as a reference.

2.3. Synthesis of 2-amino-4-(7-(diethylamino)-2-oxo-2H-chromen-3-yl)thiophene-3-carbonitrile (*CT-1*)

To a solution of **C2** (2-(1-(7-(*N*,*N*-diethylamino)-2-oxo-2H-chromen-3-yl)ethylidene)malononitrile) (10 mmol), elemental sulfur (12 mmol), and triethylamine (1 mmol) in 30 mL ethanol, were placed in a 100 mL round-bottom flask. The reaction mixture was heated under reflux with stirring for 4 h. The progress of the reaction was monitored by TLC (ethylacetate/n-hexane 1:1). After cooling, the orange precipitate was filtrated and product was washed with hot ethanol and dried. The pure

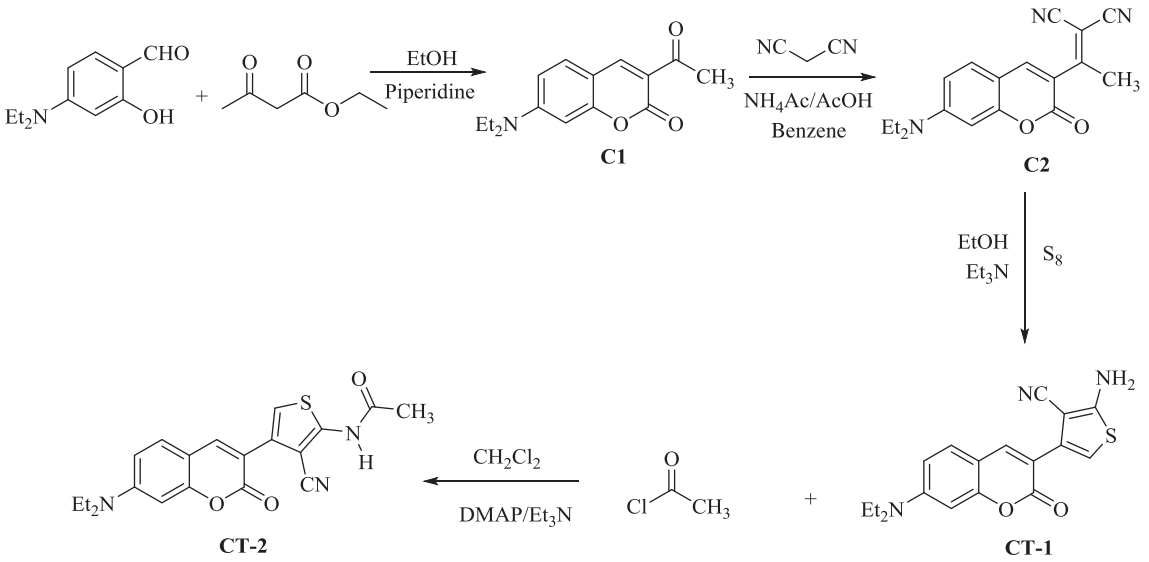

Scheme 1. Synthetic pathway for **CT-1** and **CT-2.**

Table 1
Photophysical properties of **CT-1 and CT-2**.

	CT-1				CT-2			
Solvent	λ_{abs} (nm)	λ_{fl} (nm)	Φ_{fl}	Stokes shift (nm)	λ_{abs} (nm)	λ_{fl} (nm)	Φ_{fl}	Stokes shift (nm)
DMSO	406	482	0.04	76	394	479	0.07	85
MeOH	406	514	0.02	108	404	477	–	73
CH_2Cl_2	407	464	0.60	57	408	463	0.33	55
THF	403	458	0.62	55	399	457	0.34	58
Toluene	403	447	0.74	44	402	448	–	46

Quantum yield (Φ_{fl}) of **CT-1** and **CT-2** are determined relative to the fluorescent standard coumarin 153[a]. [a]($\Phi_{fl.Cou.\ 153} = 0.38$ in ethanol).

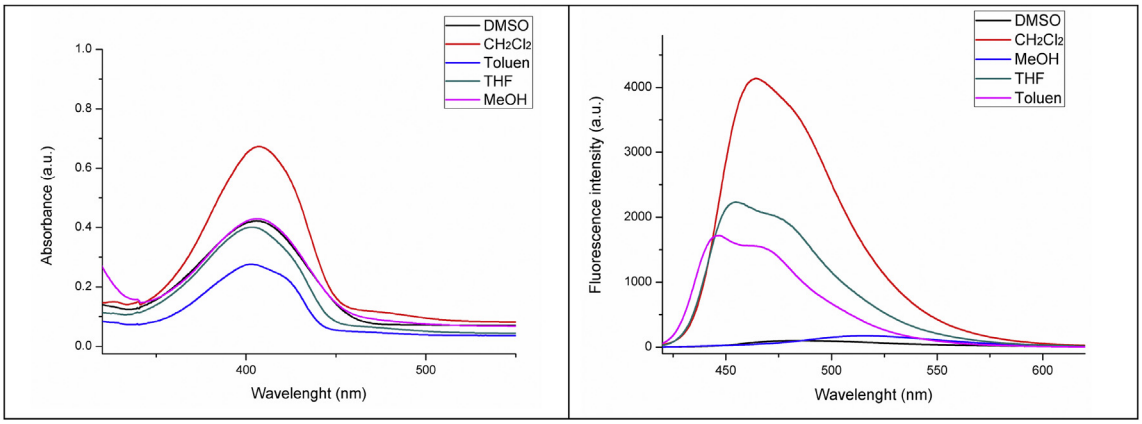

Fig. 1. UV–vis absorption spectra of **CT-1** (left). Fluorescence emission spectra of **CT-1** (right).

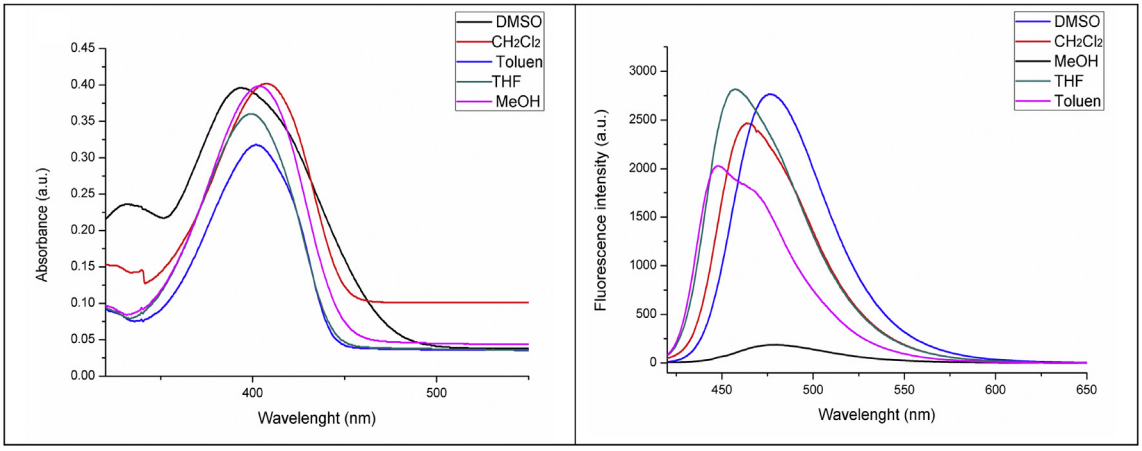

Fig. 2. UV–vis absorption spectra of **CT-2** (left). Fluorescence emission spectra of **CT-2** (right).

product was obtained as a solid after crystallization from ethanol in 78% yield. Mp: 211–213 °C. FT-IR (KBr, υ_{max}, cm^{-1}): 3395, 3322 (NH_2), 3045 (aromatic C–H), 2976 (aliphatic C–H), 2202 (CN), 1687 (C=O, lactone), 1552 (C=C), 1252 (C–O); ^{1}H NMR (DMSO-d_6, 300 MHz): δ_H 8.00 (s, 1H), 7.47 (d, 1H, $J = 8.9$ Hz), 6.72 (dd, 1H, $J = 2.2$ Hz and $J = 8.8$ Hz), 6.65 (s, 1H), 6.55 (d, 1H, $J = 2.0$ Hz), 3.50 (q, 4H, $J = 6.8$ Hz), 1.15 (q, 6H, $J = 6.9$ Hz); ^{13}C-APT (DMSO-d_6, 300 MHz): δ_C 12.8 (CH_3), 23.5 (CH_3), 44.9, 44.6 (CH_2), 84.6 (CN), 165.7 (C=O); HRMS (*m/z*), $(M + H)^+$: $C_{18}H_{13}N_3O_2S$, calculated: 340.1120; found: 340.1094.

*2.4. Synthesis of N-(3-cyano-4-(7-(diethylamino)-2-oxo-2H-chromen-3-yl)thiophen-2-yl)acetamide (**CT-2**)*

To a solution of **CT-1** (1.0 mmol), DMAP (1.7 mmol), and triethylamine (2.5 mmol) in 10 mL CH_2Cl_2, placed in a 100 mL two-neck round bottomed flask, acetylchloride (1.15 mmol) was added. The reaction mixture was stirred at room temperature for 18 h. The progress of the reaction was monitored by TLC (ethylacetate/n-hexane 1:1). After completion of the reaction, a yellow precipitate was filtrated, washed with hot CH_2Cl_2 and dried. **CT-2** was obtained in 74% yield. Mp: 340–341 °C; FT-IR (KBr, υ_{max}, cm^{-1}): 3395, 3322 (NH_2), 3045 (aromatic C–H), 2976 (aliphatic C–H), 2202 (CN), 1687

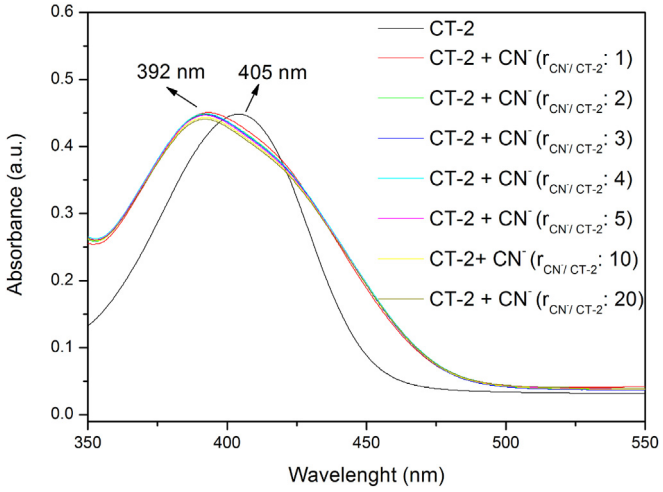

Fig. 3. UV–vis titration spectra of **CT-2** with TBACN (r:ratio).

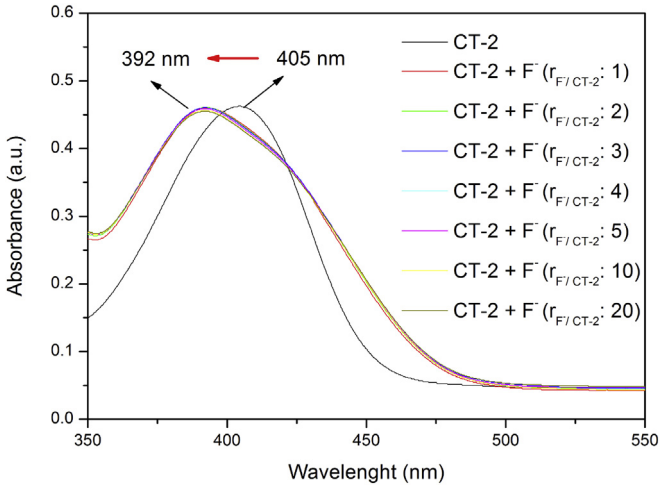

Fig. 4. UV–vis titration spectra of **CT-2** with TBAF (r:ratio).

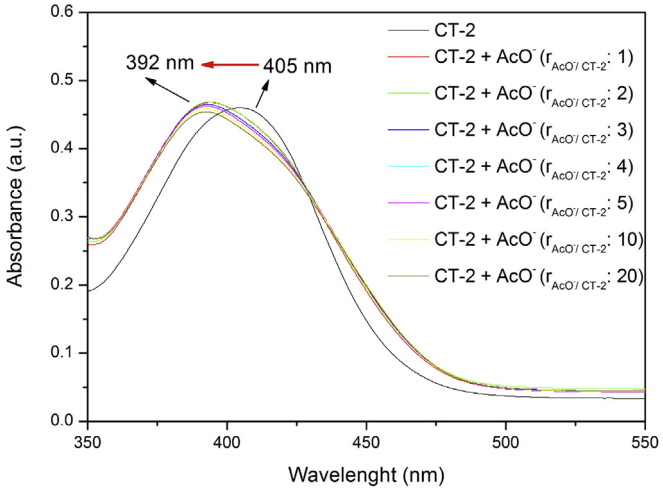

Fig. 5. UV–vis titration spectra of **CT-2** with TBAAcO (r:ratio).

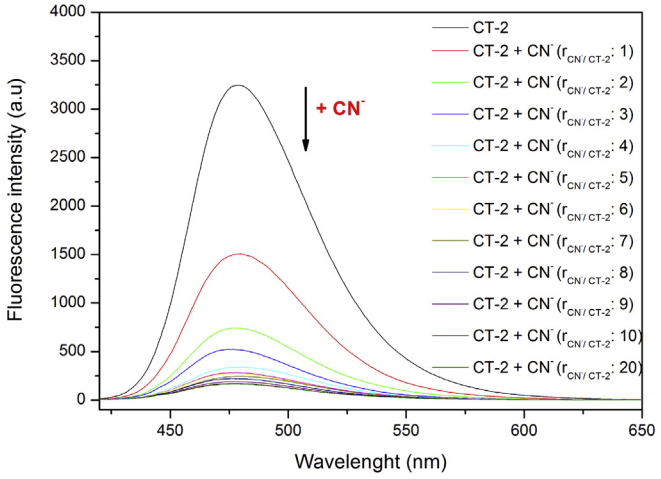

Fig. 6. Fluorescence emission titration spectra of **CT-2** with TBACN (r:ratio).

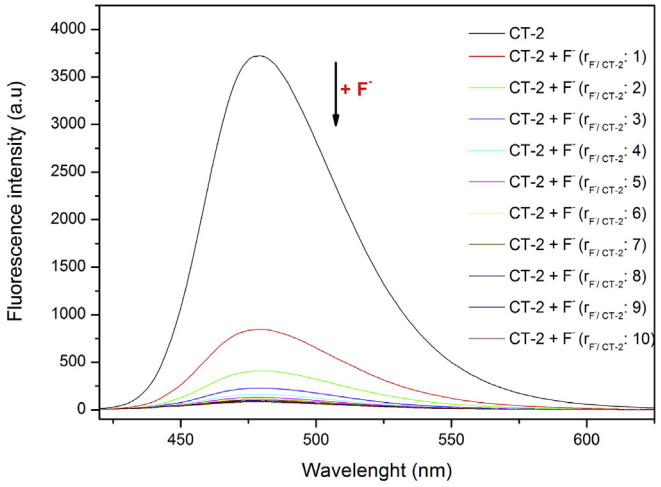

Fig. 7. Fluorescence emission titration spectra of **CT-2** with TBAF (r:ratio).

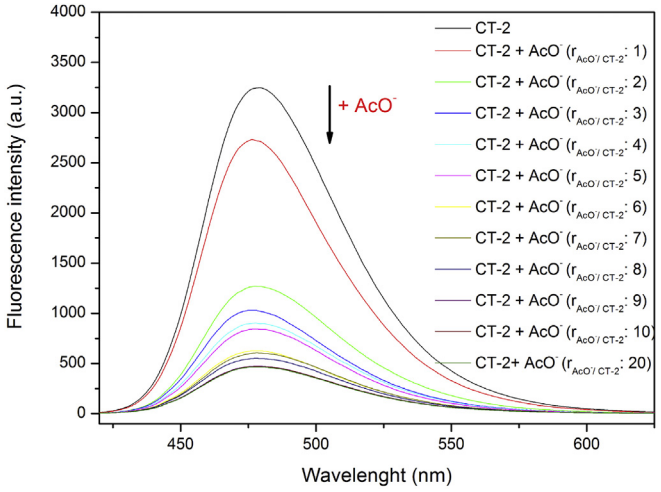

Fig. 8. Fluorescence emission titration spectra of **CT-2** with TBAAcO (r:ratio).

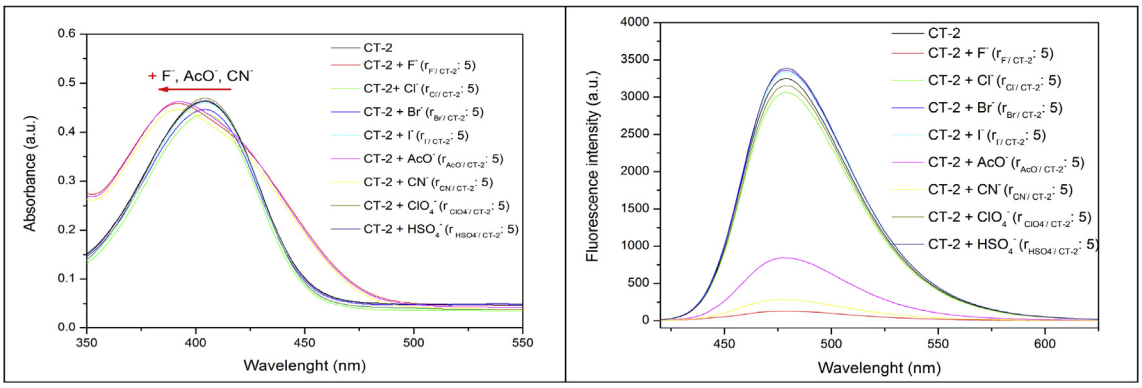

Fig. 9. Absorption (left) and emission (right) titration spectra of **CT-2** with all studied anions (r:ratio).

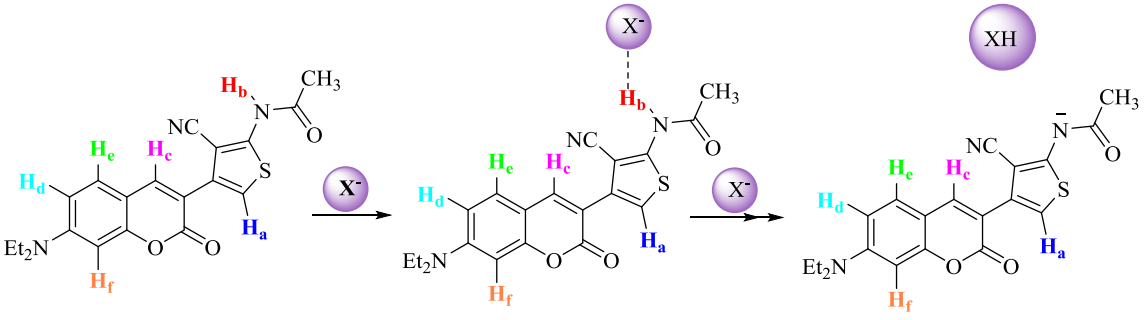

Scheme 2. Proposed binding mode of chemosensor **CT-2** with CN^-, F^- and AcO^- in DMSO solution.

(C=O, lactone), 1552 (C=C), 1252 (C–O); ^{1}H NMR (DMSO-d_6, 300 MHz) δ_H 8.02 (s, 1H), 7.45 (d, 1H, J = 8.9 Hz), 7.24 (s, 1H), 6.75 (dd, 1H, J = 2.0 Hz and J = 8.9 Hz), 6.58 (d, 1H, J = 2.0 Hz), 1.14 (q, 6H, J = 8.8 Hz); ^{13}C-APT (DMSO-d_6, 300 MHz): δ_C 12.8 (CH_3), 23.0 (CH_3), 44.6 (CH_2), 84.6 (CN), 160.2 (C=O), 169.2 (C=O); HRMS (*m/z*), $(M + H)^+$: $C_{20}H_{15}N_3O_3S$, calculated: 382.1225; found: 382,1228.

2.5. Computational details

Geometry optimizations were performed using the density functional theory (DFT) with the unrestricted formalism of B3LYP hybrid functional [17a and b,18a–f]. Pople's all-electron double-ζ basis including diffuse (+) and polarization (d,p) functions (6-31 + G(d,p)) was used [19a–e]. Harmonic vibrational frequencies were computed at the level of geometry optimization and the species reported herein were verified not to possess any imaginary frequencies, and hence correspond to true minima. Only the singlet state was considered. MO energies were reported in eV. Calculations were performed with Gaussian 09 suite of programs [20].

3. Results and discussion

3.1. Synthesis and solvatochromic properties

3-Acetyl-7-(diethylamino)-2*H*-chromen-2-one **(C1)** and 3-[7-(*N*,*N*-diethylamino)-2-oxo-2*H*-chromen-3-yl]-3-oxopropanoate (**C2**) were prepared mainly by a previously reported procedure with minor modifications (Pages S1 and S2 in Supplemantary Information) [21]. The reaction of **C2** with elemental sulfur in the presence of a catalytic amount of triethylamine in ethanol gave the fluorescent coumarin-thiophene hybrid **CT-1**. Reaction of **CT-1** with acetylchloride in CH_2Cl_2 using DMAP and triethylamine mixture yielded the desired fluorescent chemosensor **(CT-2)** (Scheme 1).

Dyes **CT-1** and **CT-2** are colored, both in solid state and in solution. In order to investigate the solvatochromic behavior, the absorption and emission data of the dyes were determined in various solvents with different dielectric constants (ε), i.e. DMSO (46.45), MeOH (32.66), CH_2Cl_2 (8.93), THF (7.58), and toluene (2.38) (Table 1).

The compounds exhibited one absorption band in all the solvents used and show absorption maxima (λ_{max}) ranging from 394 to 407 nm in the visible region. In addition, these dyes were found to be fluorescent (with emission λ_{max} 447–514 nm in all the solvent used). The compounds exhibited one emission band in all the solvents used.

The Stokes shifts of **CT-1** and **CT-2** in various solvents varied around 44–108 nm and 46–85 nm, respectively. Fluorescence quantum yields (Φ_{fl}) of **CT-1** and **CT-2** were determined in all solvent used except MeOH and Toluene for **CT-2** in the range of 0.02–0.74 (relative to commercial reference standard Coumarin 153 (0.38) (Page S11 in Supplemantary Information) (Table 1) (Figs. 1 and 2).

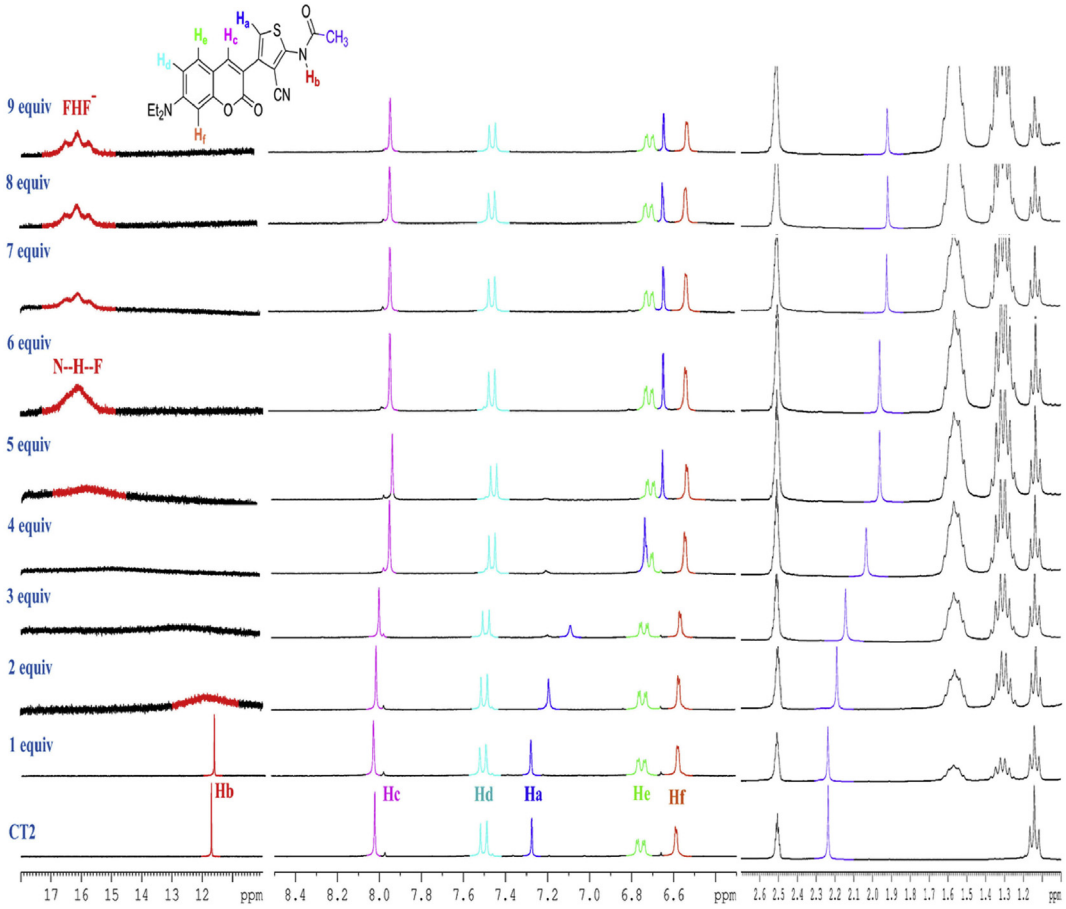

Fig. 10. ^{1}H NMR (300 MHz) titration of **CT-2** (1×10^{-2} M) with TBAF solution in DMSO-d_6.

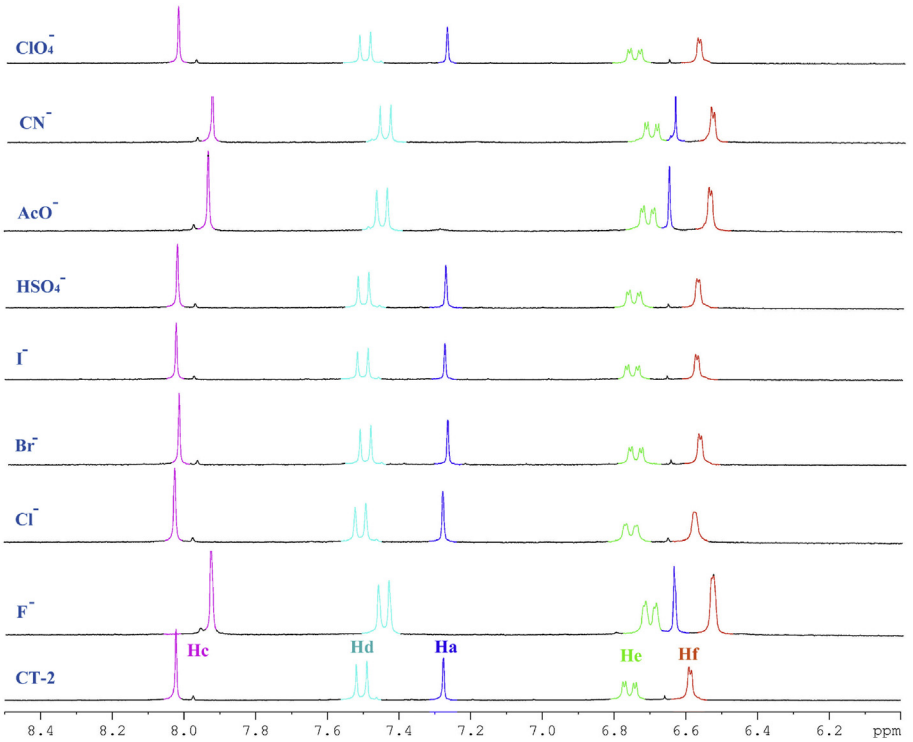

Fig. 11. Partial ^{1}H NMR (300 MHz) titration of **CT-2** (1×10^{-2} M) with studied anions ($r_{anions}/_{CT\text{-}2}$ = 1:10) solution in DMSO-d_6 (r:ratio).

3.2. UV–vis absorption and fluorescence titrations of **CT-2** with anions

The chemosensor performance of **CT-2** was investigated using UV–vis absorption and fluorescence spectroscopy in DMSO against F^-, Cl^-, Br^-, I^-, AcO^-, CN^-, HSO_4^- and ClO_4^- anions with tetrabutylammonium (TBA) as the counter cation. The absorption maximum of **CT-2** was at 405 nm in DMSO (Fig. 3**)**. This absorption band shifted hypsochromically upon addition of one equiv of CN^- to the solution of **CT-2** and a new band at $\lambda = 392$ nm was observed. Aparently, the electrostatic interaction between **CT-2** and CN^- deprotonated the amide –NH function and negative charge accumulated around the amide function giving rise to the observed hypsochromic shift. The same results were observed for AcO^- and F^- **(**Figs. 4 and 5**)**.

To gain insight into the binding nature of **CT-2** with anions, fluorescence titrations were performed in DMSO with excitation wavelength of 405 nm. Free sensor, **CT-2** displayed an emission maximum at 479 nm in DMSO with a high intensity. This UV–vis study showed that, anions such as CN^-, F^- and AcO^- can remove the –NH proton to form the corresponding anion in the ground state. Therefore, these anions were expected to induce significant fluorescence spectral changes in **CT-2**. Upon addition of CN^- (>1 equiv) to the solution of **CT-2**, the fluorescence intensity gradually decreased. Addition of 20 equiv of CN^- almost wiped out the fluorescence of **CT-2** (Fig. 6**)**. Similar results were observed for AcO^- and F^- **(**Figs. 7 and 8 in Supplemantary Information).

Interactions of **CT-2** with Cl^-, Br^-, I^-, HSO_4^- and ClO_4^- anions were also investigated by spectrophotometric and fluorimetric titrations. As shown in Fig. 9, addition of 5 equiv of these anions to the solution of **CT-2** did not result in any significant changes in the absorption and emission spectra.

The interaction between **CT-2** and the anions (F^-, Cl^-, Br^-, I^-, HSO_4^-, CN^-, AcO^-, $H_2PO_4^-$ and ClO_4^-) were probed with ^1H NMR. **CT-2** and F^- showed a clear interaction in the ^1H NMR titration of **CT-2** with TBAF solution in DMSO. The free sensor **CT-2** exhibited a sharp singlet signal at 11.68 ppm, which was assigned to amide –NH (Hb). Upon addition of 3 equiv of F^- to the solution of **CT-2**, the signal of the amide –NH proton completely disappeared due to F^- interacting with the receptoric amide moiety (Scheme 2**)**.

Upon addition of 7 equiv of F^-, the proton signals of the aromatic thiophene ring (Ha) and acetyl CH_3 shifted up-field from 7.27; 2.23 ppm to 6.64; 1.91 ppm, respectively, suggesting an accumulation of negative charge on the amide nitrogen. Thus addition of 7 equiv of F^- resulted in deprotonation and led to an increase in the electron density on the thiophene ring. Ha proton showed a drastic downfield shift due to the shielding effect of the negative electron delocalization on the π-conjugated thiophene framework. Most importantly, a new signal at 15.55 ppm ($J_{HF} = 121$ Hz) after addition of 7 equiv of F^- was observed indicating the creation of bifluoride (FHF^-) ion. Thus FHF^- was generated through abstraction of the –NH proton by F^- (Fig. 10). The same deprotonation behaviour was observed for AcO^- and CN^-, upon addition of 6 and 2.5 equiv of these anions respectively **(**Scheme 2**)**. –NH (Hb) proton signal disappeared after the addition of 1 equiv of CN^- and 2 equiv of AcO^-. This difference is probably due to the basicity and molecular shape differences of AcO^- and CN^- compared to F^- (Figs. S15 and S16 in Supplemantary Information).

For the rest of the anions (Cl^-, Br^-, I^-, $H_2PO_4^-$, HSO_4^- and ClO_4^-), even with 10 equiv, no significant changes were observed for the

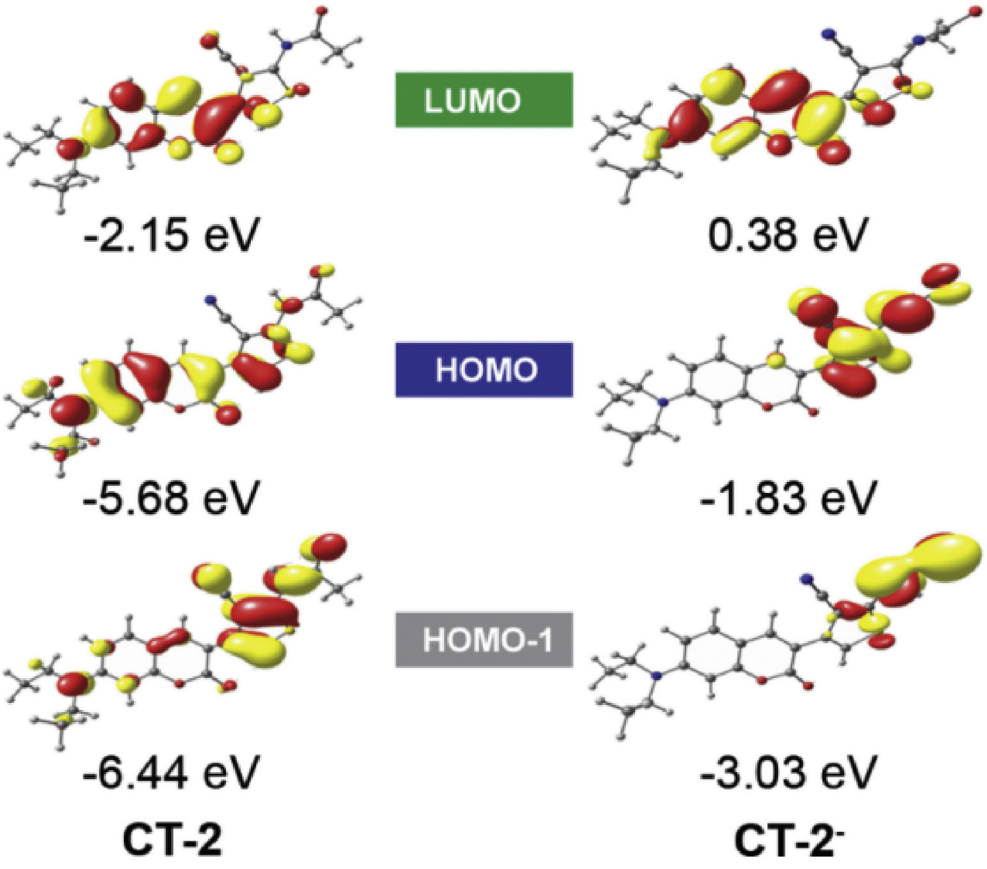

Fig. 12. Frontier orbital energies (eV) and plots (isosurface at 0.03) of **CT-2** and **CT-2**$^-$ at (U)B3LYP/6-31 + G(d,p) level of theory. Hydrogens are excluded for clarity.

aromatic thiophene proton signal (Ha). See Fig. 11 for a summary of the associated spectral changes.

3.3. Analysis of frontier molecular orbitals

We have previously shown that molecular orbital (MO) analysis is a very valuble tool to understand fluorescence switching [22]. MOs for **CT-2** and its unprotonated form (**CT-2**$^-$) are depicted in Fig. 12. (Fig. S17 in Supplemantary Information). It is clear that without the abstraction of the amide proton, **CT-2** undergoes a coumarin based $\pi \rightarrow \pi^*$ type of excitation. On the other hand, when the reseptoric amide proton is transferred to fluoride, the remaining negatively charged species is left with a large electron density accumulating on the amide nitrogen and thiophene ring. This rise in electron density, is in perfect agreement with ^{1}H NMR results, and switches the associated MO to be the HOMO in **CT-2**$^-$ instead of coumarin based HOMO in **CT-2**. Consequently while the $\pi \rightarrow \pi^*$ transition on coumarin is the electronic reason for fluorescent emission of **CT-2**, the donor to acceptor charge transfer transition quenches the fluorescence.

3.4. Thermal stability of dyes

The synthesized compounds in this study, **CT-1** and **CT-2**, are fluorescently active dyes and have potential for usage as fluorescent emitters. The light emitting potential of these dyes in the solid state is linked to their thermal stability, thus **CT-1** and **CT-2** were subjected to thermogravimetric analysis (TGA). The change in weight of the compounds was measured as a function of temperature. Thermal stability of the dyes is shown in Fig. 13. The absence of weight loss up to 80 °C indicates that no water molecules are present in the solid state. The initial decomposition temperatures (T_d) for **CT-1** and **CT-2** were found to be 324 and 344 °C respectively. Therefore, up to 320 °C, both fluorescent dyes are fairly stable and hence promising in potential optical applications.

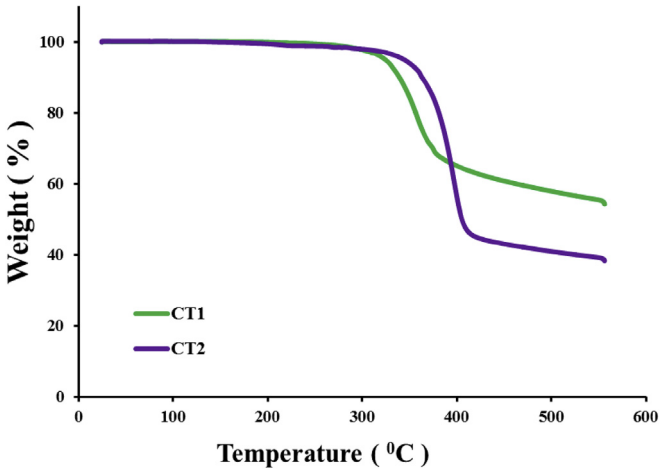

Fig. 13. TGA curves of **CT-1** and **CT-2**.

4. Conclusions

In this study, a novel coumarin-thiophene based colorimetric and fluorimetric chemosensor **(CT-2)** was successfully synthesized from coumarine-aminothiophene hybrid **(CT-1)** for ratiometric sensing of CN^-, F^- and AcO^-. The results showed that strong, visible colorimetric changes and emission quenching were observed in **CT-2** in the presence of CN^-, F^- and AcO^- in polar aprotic DMSO. However, the chemosensor was more sensitive to CN^-, than F^- and AcO^- at the stochiometric ratio of 1:2.5 respectively. The addition of CN^-, F^- and AcO^- anions resulted in a light yellow-to-deep yellow color change and emission quenched. Quantum chemical calculations suggested that fluorescence quenching is due to intramolecular charge transfer. No significant color or emission changes were observed with the naked eye upon addition of the rest of the ions (Figs. 14 and 15). Additionally, the TGA results show that the dyes **CT-1** and **CT**-2 have an enough thermal stability for optical applications.

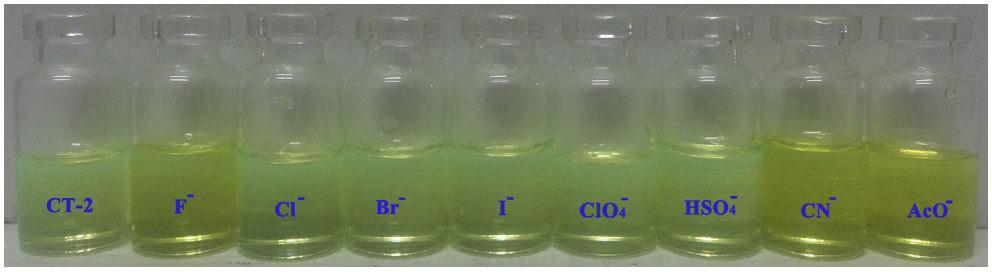

Fig. 14. 1×10^{-3} M solutions of **CT-2** in DMSO under ambient light, ($r_{Anion/CT\text{-}2}$:10).

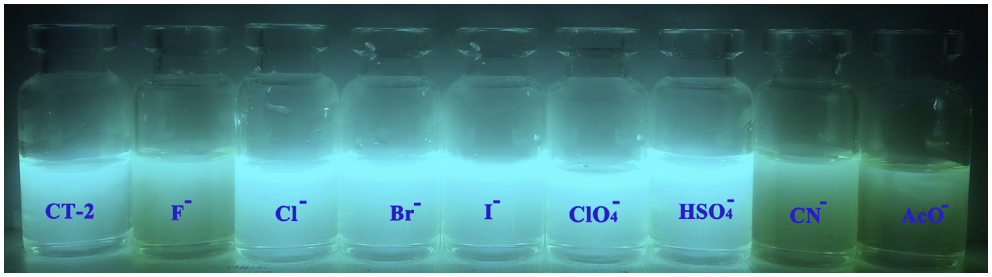

Fig. 15. 1×10^{-3} M solutions of CT-2 in DMSO under UV light, 365 nm, (rAnion/CT-2:10).

Acknowledgements

We are grateful to The Scientific and Technological Research Council of Turkey for providing financial support (Project Grant No: 114Z980) for this study.

Appendix A. Supplementary data

Supplementary data related to this article can be found at http://dx.doi.org/10.1016/j.molstruc.2015.11.081.

References

[1] P.D. Beer, P.A. Gale, Anion recognition and sensing: the state of the art and future perspectives, Angew. Chem. Int. Edi 4 (2001) 486–516.
[2] S. Ayoob, A.K. Gupta, Fluoride in drinking water: a review on the status and stress effects, Crit. Rev. Env. Sci. Technol. 36 (2006) 433–487.
[3] K.L. Kirk, Biochemistry of the Halogens and Inorganic Halides, Plenum Press, New York, 1991, p. 58.
[4] M. Kleerekoper, The role of fluoride in the prevention of osteoporosis, Endocrin Metab. Clin. 27 (1998) 441–452.
[5] C.D. Geddes, Optical halide sensing using fluorescence quenching theory simulations and applications-a review, Meas. Sci. Technol. 12 (2001) 53–88.
[6] A. Graefe, S.E. Stanca, S. Nietzsche, L. Kubicova, R. Beckert, C. Biskup, G.J. Mohr, Development and critical evaluation of fluorescent chloride nanosensors, Anal. Chem. 80 (2008) 6526–6531.
[7] B. Ma, F. Zeng, F. Zheng, S. Wu, A fluorescence turn-on sensor for iodide based on a Thymine–HgII–Thymine complex, Chem. Eur. J. 17 (2011) 14844–14850.
[8] M. Haldimann, B. Zimmerli, C. Als, H. Gerber, Direct determination of urinary iodine by inductively coupled plasma mass spectrometry using isotope dilution with iodine-129, Clin. Chem. 44 (1998) 817–824.
[9] W. Huang, Z. Chen, H. Lin, H. Lin, A novel thiourea–hydrazone-based switch-on fluorescent chemosensor for acetate, J. Lumin 131 (2011) 592–596.
[10] J. Shao, H. Lin, M. Yu, Z. Cai, H. Lin, A simple and efficient colorimetric anion sensor based on a thiourea group in DMSO and DMSO–water and its real-life application, Talanta 75 (2008) 551–555.
[11] R.M. Manez, F. Sancenon, Fluorogenic and chromogenic chemosensors and reagents for anions, Chem. Rev. 103 (2003) 4419–4476.
[12] N. Kumari, S. Jha, S. Bhattacharya, Colorimetric probes based on anthraimidazolediones for selective sensing of fluoride and cyanide ion via intramolecular charge transfer, J Org. Chem. 76 (2011) 8215–8222.
[13] L. Long, X. Li, D. Zhang, S. Meng, J. Zhang, X. Sun, C. Zhang, L. Zhou, L. Wang, Amino-coumarin based fluorescence ratiometric sensors for acidic pH and their application for living cells imaging, RSC Adv. 3 (2013) 12204–12209.
[14] L. Long, L. Zhou, L. Wang, S. Meng, A. Gong, F. Dub, C. Zhang, A coumarin-based fluorescent probe for biological thiols and its application for living cell imaging, Org. Biomol. Chem. 11 (2013) 8214–8220.
[15] G.A. Crosby, J.N. Demas, Measurement of photoluminescence quantum yields, Rev. J. Phys. Chem. 75 (1971) 991–1024.
[16] B. Valeur, Molecular Fluorescence, Wiley-VCH Verlag GmbH, Weinheim, 2002.
[17] (a) W. Kohn, A.D. Becke, R.G. Parr, Density functional theory of electronic structure, J. Phys. Chem. 100 (1996) 12974–12980;
(b) R.G. Parr, W. Yang, Density Functional Theory of Atoms and Molecules, Oxford University Press, New York, 1989.
[18] (a) S.H. Voskon, L. Wilk, M. Nusair, Accurate spin-dependent electron liquid correlation energies for local spin density calculations: a critical analysis, Can. J. Phys. 58 (1980) 1200–1211;
(b) A.D. Becke, Density-functional exchange-energy approximation with correct asymptotic behavior, Phys. Rev. A 38 (1988) 3098;
(c) C.T. Lee, W.T. Yang, R.G. Parr, Development of the Colle-Salvetti correlation-energy formula into a functional of the electron density, Phys. Rev. B 37 (1988) 785–789;
(d) A.D. Becke, Density-functional thermochemistry. III. The role of exact exchange, J. Chem. Phys. 98 (1993) 5648–5652;
(e) P.J. Stephens, F.J. Devlin, C.F. Chabalowski, M.J. Frisch, Ab initio calculation of vibrational absorption and circular dichroism spectra using density functional force fields, J. Phys. Chem. 98 (1994) 11623–11627;
(f) R.H. Hertwig, W. Koch, On the parameterization of the local correlation functional. what is Becke-3-LYP? Chem. Phys. Lett. 268 (1997) 345–351.
[19] (a) M.J. Frisch, J.A. Pople, J.S. Binkley, Self-consistent molecular orbital methods 25. Supplementary functions for Gaussian basis sets, J. Chem. Phys. 80 (1984) 3265–3269;
(b) T. Clark, J. Chandrasekhar, G.W. Spitznagel, P.R. Schleyer, Efficient diffuse function-augmented basis sets for anion calculations. III. The 3-21+G basis set for first-row elements, Li–F, J. Comp. Chem. 4 (1983) 294–301;
(c) W.J. Hehre, R. Ditchfield, J.A. Pople, J. Chem. Phys. 56 (1972) 2257;
(d) P.C. Hariharan, J. Pople, 6-31G basis set, Theor. Chem. Acc. 28 (1973) 213–222;
(e) P.C. Hariharan, J.A. Pople, Accuracy of AH an equilibrium geometries by single determinant molecular orbital theory, Mol. Phys. 27 (1974) 209–214.
[20] M.J. Frisch, G.W. Trucks, H.B. Schlegel, G.E. Scuseria, M.A. Robb, J.R. Cheeseman, et al., Gaussian 09, Revision A.2, Gaussian, Inc, Wallingford CT, 2009.
[21] E. Yalçın, Y.C. Kutlu, V. Korkmaz, E. Sahin, Seferoglu.,2,6-Dicyanoaniline based donor-acceptor compounds: the facile synthesis of fluorescent 3,5-diaryl/hetaryl-2,6- dicyanoanilines, Arkivoc 1 (2015) 202–218.
[22] S. Yalçın, L. Thomas, M. Tian, N. Seferuğlu, H. Ilmels, Y. Dede, Switching off the charge transfer and closing the S1–T1 ISC channel in excited states of quinolizinium derivatives: a theoretical study, J. Org. Chem. 79 (2014) 3799–3808.